

Numerical Simulation of Transient Force and Eddy Current Loss in a 720-MVA Power Transformer

S. L. Ho, Y. Li, H. C. Wong, S. H. Wang, and R. Y. Tang

Abstract—The transient eddy current fields are short-circuit forces upon the coils of large power transformers are analyzed. The proposed approach is based on the A–V–A formulation in which the eddy current field and the electric circuit equations are solved simultaneously. The effectiveness of a magnetic bypass plate near the coils ends for reducing the eddy current loss and the local overheating is discussed. A simulation to study the transient short-circuit behavior of a 720-MVA power transformer using the proposed coupled approach is reported.

Index Terms—Eddy current loss, power transformer, transient force.

I. INTRODUCTION

THE ELECTROMAGNETIC forces on the windings of large transformer due to short circuits are generally detrimental. A three-dimensional (3-D) nonlinear transient electromagnetic field is necessary when studying these transient short-circuiting forces. A transient field study using current source has been reported [1]. However, most large transformers are connected to constant voltage sources, and the short-circuit currents in the coils are unknown. Recently, there are algorithms to couple the magnetic and electric circuits in the simulation of motors [2], [3], turbo-generators, and other devices [4]–[6].

Common measures to alleviate the eddy current and overheating problems are to reduce the magnetic flux density in the metallic clamping plates and tank walls. Shields and metals with low permeability are also used to reduce the eddy current losses. However, these measures are insufficient for large transformers rated up to 720 MVA. Indeed large transformers are commonly fitted with magnetic bypass (MBP) plates near the coil ends to reduce the eddy current losses.

Unlike the normal pie windings in conventional transformers with negligible axial current and torsional forces [7], the spiral coils in large transformers may be acted upon by torsional forces due to the presence of axial component of the current. Test results show that coil damages due to torsional force are not uncommon; hence, it is necessary to calculate the distribution of torsional force on the coils.

Manuscript received July 1, 2003.

S. L. Ho is with the Department of Electrical Engineering, The Hong Kong Polytechnic University, Hong Kong (e-mail: eeslho@polyu.edu.hk).

Y. Li and R. Y. Tang are with the Research Institute of Special Electrical Machines, Shenyang University of Technology, Shenyang, 110023 China (e-mail: liyant@yahoo.com; sygdtd@mail.sy.ln.cn).

H. C. Wong is with the Industrial Center, The Hong Kong Polytechnic University, Hong Kong (e-mail: ichcwong@polyu.edu.hk).

S. H. Wang is with the Department of Electrical Engineering, Shenyang University of Technology, Shenyang, 110034 China (e-mail: wyxzy@263.net).

Digital Object Identifier 10.1109/TMAG.2004.824801

This paper presents a 3-D A–V–A coupled formulation in which the eddy current field and the electric circuit equations are solved simultaneously. Useful results on the transient short-circuit behavior of a 720-MVA power transformer windings are obtained in the simulation study.

Besides axial and radial forces, the distribution of torsional force on the spiral coils is calculated. The mechanical robustness and stability of the coil are checked. The loss density and magnetic flux density in the clamping plate with and without a magnetic bypass plate is studied and reported.

II. A–V–A COUPLED FORMULATION

A. Electromagnetic Field Equations

From Maxwell's equations, the A–V–A formulations with the Coulomb gauge can be written as [7]

$$\begin{aligned} \nabla \times \nu \nabla \times \mathbf{A} - \nabla \nu \nabla \cdot \mathbf{A} + \sigma \nabla V + \sigma \frac{\partial \mathbf{A}}{\partial t} \\ = \mathbf{t} \frac{n_c}{S_c} i(t) \quad \text{in } \Omega_1 + \Omega_2 \\ \nabla \cdot \left(-\sigma \frac{\partial \mathbf{A}}{\partial t} - \sigma \nabla V \right) = 0 \quad \text{in } \Omega_1 \end{aligned} \quad (1)$$

where Ω_1 and Ω_2 are, respectively, the region with and without eddy currents, \mathbf{A} is the magnetic vector potential, ν is the reluctivity tensor, σ is the conductivity tensor, V is the electric scalar potential, \mathbf{t} is a unit coil direction field vector tangential to the windings, n_c is the number of turns, S_c is the total cross-sectional area of the windings, and $i(t)$ is the current per turn.

The matrix of the field equation system can be written as

$$[\mathbf{K}]\{\mathbf{A}_v\} + [\mathbf{M}]\frac{\partial}{\partial t}\{\mathbf{A}_v\} - [\mathbf{C}]\{\mathbf{I}\} = 0 \quad (2)$$

where $\{\mathbf{A}_v\} = [A_x A_y A_z V]^T$. Equation (2) is the conventional formulation where the current is used as the input.

B. Equations of the Electric Circuit

Power transformers connected to voltage sources are characterized by the following circuit equation:

$$u = \frac{n_c}{S_c} \frac{\partial}{\partial t} \int_{\Omega} \mathbf{A} \cdot \mathbf{t} d\Omega + Ri + L \frac{di}{dt} \quad (3)$$

where Ω is the space filled with windings. Moreover, the matrix equation of the equivalent circuit can be written as

$$[\mathbf{C}]^T \frac{\partial}{\partial t} \{\mathbf{A}_v\} + [\mathbf{L}] \frac{d}{dt} \{\mathbf{I}\} + [\mathbf{R}]\{\mathbf{I}\} = [\mathbf{u}] \quad (4)$$

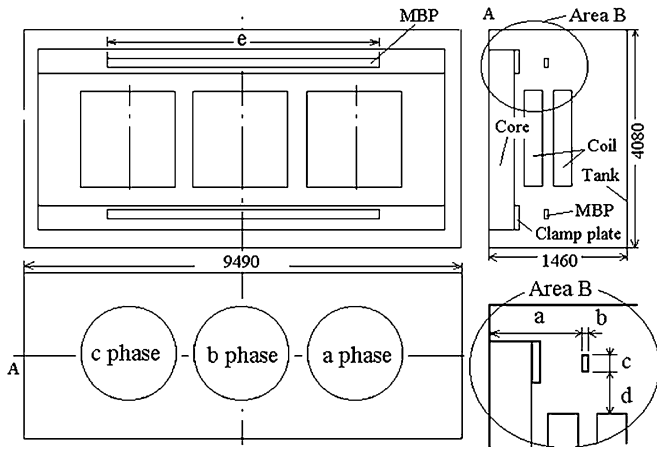


Fig. 1. Sketch of transformer with magnetic bypass plates.

TABLE I
COMPARISON BETWEEN COMPUTED AND MEASURED MAXIMUM
MAGNETIC FLUX DENSITY (mT)

Height (mm)	442	597	900	1057	1125	1198
Computed	6.64	4.87	4.71	2.91	5.66	9.87
Experimental	6.1	4.98	4.62	3.10	6.35	9.05
Error (%)	9.6	-1.6	1.1	-9.4	-12.8	8.7

C. Magnetic Field and Electric Circuit Coupled Equations

Equations (2) and (4) give the following coupled equation:

$$\begin{bmatrix} K & -C \\ 0 & R \end{bmatrix} \begin{Bmatrix} \mathbf{A}_v \\ \mathbf{I} \end{Bmatrix} + \begin{bmatrix} M & 0 \\ C^T & L \end{bmatrix} \frac{d}{dt} \begin{Bmatrix} \mathbf{A}_v \\ \mathbf{I} \end{Bmatrix} = \begin{Bmatrix} 0 \\ \mathbf{u} \end{Bmatrix} \quad (5)$$

The Newton-Raphson algorithm is used to take into account of the magnetic nonlinearity.

III. ANALYSIS AND CALCULATION

Equations (1)–(5) are employed to compute the transient eddy current fields and the electromagnetic forces upon the coils in a 720-MVA/500 kV transformer. Fig. 1 shows a sketch of the structure of a transformer with a magnetic bypass plate.

To validate the approach presented in this paper, a 17-MVA transformer is selected as the magnetic field test model. The corresponding calculated values of magnetic flux density on the surface of the iron core and the tested results are given in Table I, which shows that the calculated results agree well with the measured ones. For electric equations with known terminal voltages, the coupled method is the most suitable one for transient analyses of the transformer.

As it is difficult to measure the short-circuit (SC) forces of the 720-MVA power transformer, the short-circuit tests have been done on two smaller transformers. The forces on the up yoke of the iron core are measured by using pressure force sensors between the press plate and the clamp plate. Table II shows the computed and tested results.

The primary short-circuit currents are shown in Fig. 2. It can be seen that the current computed using traditional method in which the inductance and the resistance of the transformer are treated as constants is slightly larger than that obtained from the field-circuit coupled method, which has a maximum current error of about 16.7%.

TABLE II
SC FORCE ACTING ON THE UP YOKE OF CORE

Transformer model	The SC force acting on the up yoke (10^4 N)		
	Computed	Tested	Error (%)
8000kVA	9.7	11.1	-12.6
31500kVA	34.5	38.0	-9.26

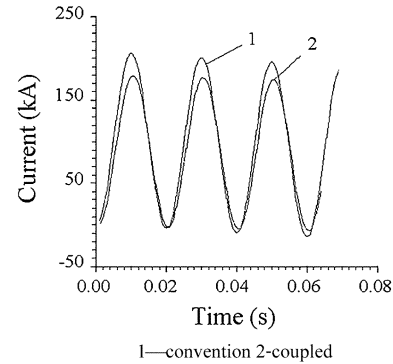


Fig. 2. Primary short-circuit currents.

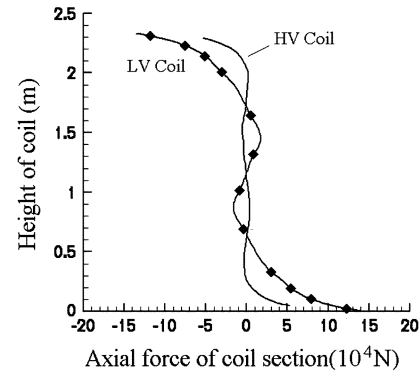


Fig. 3. Distribution of axial forces of coil-sections.

A. Short-Circuit Forces on the Coils

The mechanical strength of the high voltage (HV) coil and the mechanical stability of the low voltage (LV) coil are key indicators in assessing the robustness of the transformer against short-circuit damages. Hence, the distribution of the forces on the coils and the time variation of the forces have to be computed for subsequent mechanical analysis. Fig. 3 depicts the distributions of the axial electromagnetic force of the coil sections in the B-phase LV and HV coils along the z direction (height of the coil). From Fig. 3 it can be seen that axial forces of sections near the end regions of the coils are larger than those near the middle of the coils because of the radial magnetic flux density and the nonuniform distribution of ampere-turns along the height of coils. Fig. 4 gives the distribution of radial forces on the coil sections.

In general, most power transformers are studied as pie coil models with no axial short-circuit current. Unlike traditional ones, the 720-MVA transformer uses spiral coils with axial currents. Fig. 5 shows the distributions of the torsional force on the B-phase LV coil along the z direction (height of coil). It can be seen that the torsional force of the coil sections near the end region of the windings is larger than those near the middle.

In order to study the behavior of the coils due to the short-circuit forces, it is necessary to check the mechanical robustness

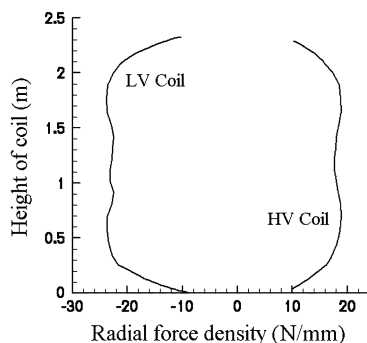


Fig. 4. Distribution of the radial forces on the B-phase coils along the height of the coils.

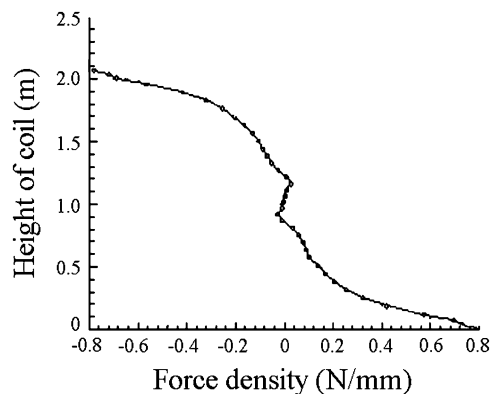


Fig. 5. Distribution of the torsional force on the B-phase low-voltage coil along the z direction (height of coil).

and stability of the coils. To calculate the mechanical stress of the HV coil, the coil is simplified as a ring model with uniform circumferential supporting bars as well as cushion blocks and space beam elements to describe the model. If the maximum radial forces of the HV coil sections are assumed as static load, the static mechanical strength analysis can be carried out. The computed maximum static stress is 85 MPa, which acts on a coil section at a location with a height of 1280 mm on the coil.

Besides the maximum static stress, the dynamic stresses of the coil sections need to be analyzed too. In the short-circuit test of a large power transformer, the test time is usually 200 ms. In the dynamic mechanical strength analysis, the stress of the coil sections during the test must be determined. Fig. 6 gives the maximum stress of the HV coil sections along the z direction of the coil. The maximum dynamic stress is 59.6 MPa, which is less than the allowable stress of 100–160 MPa for the copper wire in the coil. Hence, the test shows that the coils do have sufficient mechanical rigidity to withstand the short-circuit impacts. Fig. 7 shows the time variation of the stress of one coil section at a height of 1280 mm on the B-phase HV coil.

For low-voltage coils, the maximum radial force of the coil sections in the transformer is 23 207 N/m, which is less than collapsing critical force of 36 355 N/m in the radial direction. Hence, there is no radial destabilization danger for the coil.

B. Eddy Current Field Calculation

Due to transportation constraints, the physical size of the 720-MVA transformer is very compact, and hence, its electromagnetic load density is very large. The field will induce

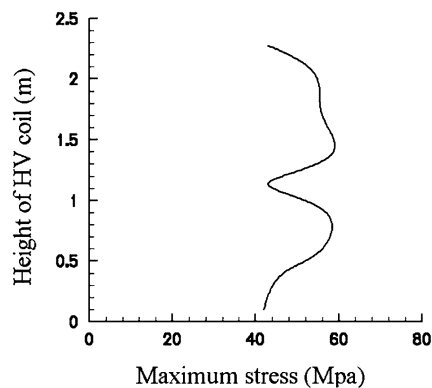


Fig. 6. Maximum stress of the HV coil sections.

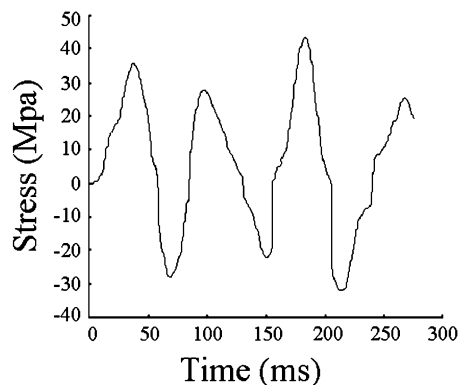


Fig. 7. Time variation of the stress of a coil section 1280 mm in height of the B-phase HV coil.

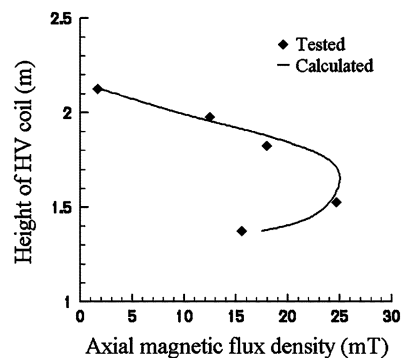


Fig. 8. Field distribution on the outside surface of the HV coil.

not only heavy eddy current loss in some metal parts of the transformer such as in the clamp plates, tank wall and so on, but it also gives rise to local overheating problems. In the transformer, all the clamp plates are made of the steel with low magnetic permeability in order to alleviate the problem. In order to obtain an accurate distribution of the leakage magnetic field in the 720-MVA transformer, some tests have been done in which the electromagnetic fields on the outside surface of the C-phase HV coil, on the up clamp and on the inside surface of the tank wall have been measured. In the region of the clamp plate corresponding to the center lines of C-phase coils, the maximum B_z is 126 mT, which is larger than the critical overheating criterion value of 26.7 mT. The maximum loss density is 46 kW/m³ before installing the MBP plates. In the single-phase transformer model of the 720-MVA

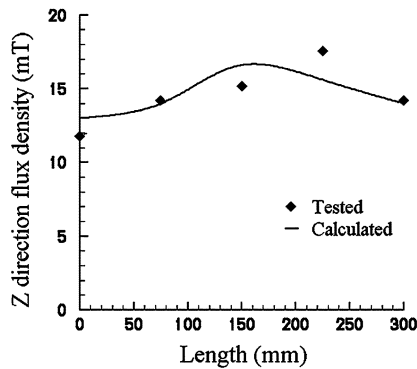


Fig. 9. Magnetic flux density B_z on the area of the up clamp plate.

TABLE III
LOSS DENSITY IN THE CLAMPING PLATE

Length of clamp	0	0.5	1.0	1.5	2.0	2.5	3.0	3.5	4.0
Loss density 1	1.3	1.8	2.2	2.1	1.8	1.3	1.4	1.3	1.1
Loss density 2	40.5	35.1	20.2	14.3	20.1	31.0	39.5	30.2	20.5

transformer, the overheating problem in the clamp plates has been measured using infrared radiation thermometer. Besides using low magnetic permeability steel clamp plates, a magnetic bypassing plate scheme is designed to reduce the losses of the clamp plates to solve the local overheating problem. The MBP plates, which are made of silicon sheets, are installed near the clamp plates so as to provide a path for the leakage magnetic field at the end of the three phase coils in the MBP plates. The leakage magnetic field in the clamp plates, pull plates and so on can be reduced with this arrangement.

Fig. 8 gives the field distribution on the outside surface of the HV coil. Fig. 9 shows the distribution of the z direction magnetic flux density B_z along the length direction of the up clamp plate. The analyzed area is corresponding to a region of the C-phase coil. Because the maximum magnetic flux density is 16.6 mT, which is less than the aforementioned criterion after installing the MBP plates, there is no local overheating in the clamp plates. Meanwhile, the maximum loss density is reduced to 2.2 kW/m³. The calculated results of the magnetic flux density in the up clamp plate is observed to agree well with the test results. By optimizing the parameters of the MBP plate, such as a , b , c , d , and e in Fig. 1, the maximum loss density in the plates can be reduced by 94%. In this scheme, $a = 947$ mm, $b = 50$ mm, $c = 80$ mm, $d = 205$ mm, and $e = 8800$ mm. Table III gives a comparison of the loss density in the clamp plate from the middle to the end along the axial direction. The MBP plate is effective to reduce the losses of these parts to avoiding local overheating problem.

In computing the electromagnetic field of the MBP plates, the maximum magnetic flux density is found to be 1.35 T and that is less than the saturation flux density. Moreover, the measured value is 1.23 T and this compares well with the computed one. The eddy current loss in the MBP plate is small because they are made of silicon sheets. The design of the MBP plates is thus successful. Fig. 10 gives the distribution of the magnetic field in the up MBP plate.

As the loss in the tank wall is high, a 4-mm-thick copper shield is used to alleviate the overheating problem in the tank



Fig. 10. Distribution of the magnetic field in the up MBP plate.

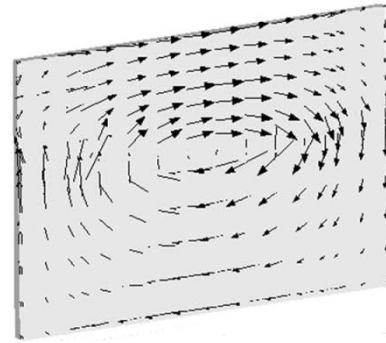


Fig. 11. Distribution of eddy current density in the tank wall.

wall. The total losses in the copper shield and tank wall is then reduced by 80% as compared to that with an unshielded tank wall. Meanwhile, the maximum loss density is reduced from 200 kW/m³ to 25 kW/m³. Fig. 11 gives the distribution of the eddy current density in the tank wall.

IV. CONCLUSION

This paper presents a 3-D A-V-A coupled formulation in which the eddy current field and the electric circuit equations in a power transformer are solved simultaneously.

Besides axial and radial forces, the torsional force acting on the spiral coils is computed. By checking the mechanical robustness and stability of the coil, one can evaluate whether the coils can withstand the short-circuit forces.

By optimizing the magnetic bypass plate, the losses are reduced significantly, and hence, overheating in the clamping plates is avoided.

REFERENCES

- [1] Y. Li *et al.*, "Analyses of transient force of coils in large transformers," in *Proc. CICEM*, 1999, pp. 406–409.
- [2] E. G. Strangas, "Coupling the circuit equations to the nonlinear time dependent field solution in inverter driven induction motors," *IEEE Trans. Magn.*, vol. 21, pp. 2408–2411, Nov. 1985.
- [3] A. Bossavit, "Time-stepping finite element analysis of induction motor," in *Proc. ICEM*, 1988, pp. 275–280.
- [4] F. Piriou and R. Razek, "Coupling of saturated electromagnetic systems to nonlinear power electric devices," *IEEE Trans. Magn.*, vol. 24, pp. 274–277, Jan. 1988.
- [5] A. Nicolet, F. Delince, N. Bamps, A. Grenon, and W. Legros, "A coupling between electric circuit and 2D magnetic field modeling," *IEEE Trans. Magn.*, vol. 29, pp. 1697–1699, Mar. 1993.
- [6] T. Derher and G. Meunier, "3D modeling of electromagnets fed by alternating voltage sources," *IEEE Trans. Magn.*, vol. 29, pp. 1341–1344, Mar. 1993.
- [7] R. Y. Tang, "Transient simulation of power transformers using 3D finite element model coupled to electric circuit equations," *IEEE Trans. Magn.*, vol. 36, pp. 1417–1420, July 2000.
- [8] Y. Q. Tang *et al.*, "Numerical calculation of short circuit electromagnetic forces on the transformer winding," *IEEE Trans. Magn.*, vol. 26, pp. 1039–1041, Mar. 1990.